Journal of the Korean Society of Marine Environment & Safety
Research Paper
Vol. 24, No. 3, pp. 325-331, May 31, 2018, ISSN 1229-3431(Print) / ISSN 2287-3341(Online) https://doi.org/10.7837/kosomes.2018.24.3.325

Dynamical Rolling Analysis of a Vessel in Regular Beam Seas

Sang-Do Lee* · Sam-Sang You**†

* Graduate School of Korea Maritime and Ocean University, Busan, Korea
** Division of Mechanical Engineering, Korea Maritime and Ocean University, Busan, Korea

Abstract : *This paper deals with the dynamical analysis of a vessel that leads to capsize in regular beam seas. The complete investigation of nonlinear behaviors includes sub-harmonic motion, bifurcation, and chaos under variations of control parameters. The vessel rolling motions can exhibit various undesirable nonlinear phenomena. We have employed a linear-plus-cubic type damping term (LPCD) in a nonlinear rolling equation. Using the fourth order Runge-Kutta algorithm with the phase portraits, various dynamical behaviors (limit cycles, bifurcations, and chaos) are presented in beam seas. On increasing the value of control parameter Ω, chaotic behavior interspersed with intermittent periodic windows are clearly observed in the numerical simulations. The chaotic region is widely spread according to system parameter Ω in the range of 0.1 to 0.9. When the value of the control parameter is increased beyond the chaotic region, periodic solutions are dominant in the range of frequency ratio Ω=1.01~1.6. In addition, one more important feature is that different types of stable harmonic motions such as periodicity of 2T, 3T, 4T and 5T exist in the range of Ω=0.34~0.83.*

Key Words : *Nonlinear dynamical behavior, Rolling motion, Bifurcation, Chaos, Limit cycle, Sub-harmonics*

1. Introduction

Unexpected rolling motion poses serious problems to the safe navigation of vessels. It is well known that the rolling motion of vessels show strong nonlinear dynamical behaviors. Harmonic, sub-harmonic, limit cycle and chaotic motions may occur even in regular beam seas. One of the important properties of chaos is dynamical sensitivity depending on initial conditions. Therefore, nonlinear behaviors of rolling motion should be examined in detail since it can drastically affect vessel motions.

because the vessel motions can be changed drastically.

It is noted that the sub-harmonic frequencies are frequencies below the fundamental frequency of an oscillator in a ratio of $1/n$, with n a positive integer. If $n(>1)$ is an integer, the period is the time interval (sec) required to travel $2\pi n$ (rad) instead of 2π (rad). Then the system response is said to be a sub-harmonic of order $1/n$ (Jordan and Smith, 2007). Forced rolling motion with nonlinear restoring moments may have frequencies lower than the encountering frequency. This is known as sub-harmonic oscillations (Bhattacharyya, 1978).

Nonlinear dynamical behaviors of a vessel rolling under external excitations have been investigated in the past years. With experimental methods, Francescutto and Contento (1999) also studied the steady rolling responses for a scale model of a destroyer in regular beam seas. Using a generalized Melnikov's method and Markov approach, Lin and Yim (1995) investigated the qualitative behavior of the chaotic motion and capsizing of a vessel in probability space. They developed a stochastic analysis procedure to examine the periodic, chaotic and capsizing responses of a vessel's rolling motion with random noises and disturbances. Melnikov's method is widely used to determine the existence of homoclinic orbits in the vector field (roll angle and rate). Wu and MeCue (2008) applied the extended Melnikov's method to analyze the rolling motion without the constraint of small damping term.

In special cases, it is reasonable to think that the rolling motion can be uncoupled and the center of the coordinate is located at the roll center (Roberts and Vasta, 2000). Neves et al. (1999) experimentally studied the effects of the heave and pitch motion of fishing vessels in longitudinal waves. Kamel (2007) investigated the bifurcation analysis of a coupled pitch-roll (2DOF) vessel motions with quadratic coupling. Similarly, Zhou and Chen (2008) considered a vessel with nonlinear coupled pitch and roll modes. Sayed and Hamed (2011) also dealt with a coupled pitch-roll vessel motions using the averaging method.

This paper considers the vessel rolling motions governed by a single-degree-of-freedom (SDOF) equation. Nonlinear rolling dynamics including sub-harmonic and chaotic motions of a vessel in beam waves are extensively investigated. Bifurcation analysis has been employed to examine the ranges in detail where

* First Author : oksangdo@naver.com
† Corresponding Author : ssyou@kmou.ac.kr, 051-410-4366

nonlinear phenomena are observed under the variations of control parameters. Bifurcation is one of the important characteristics for dynamical analysis. It can provide models of transitions and instabilities as some control parameters are varied (Strogatz, 1994).

2. Mathematical Formulation

2.1 System description

For undamped or proportionally damped systems, vessel rolls about a roll center, like a pendulum, can be decoupled from sway (Wang, 2010). As depicted in Fig. 1, for the body frame (X, Y, Z), the vessel is constrained to rotate in a one dimensional motion about the roll axis (X) through its center of gravity (G).

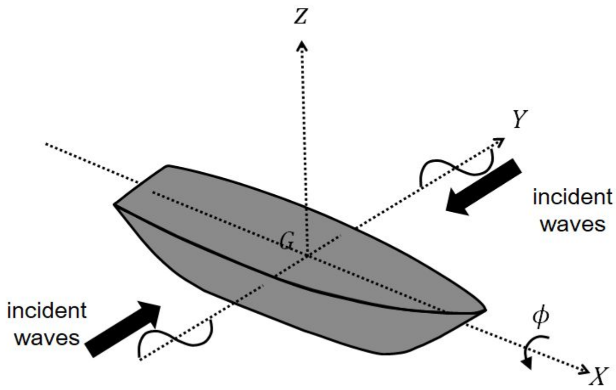

Fig. 1. Roll motion of a vessel in regular beam seas.

In general, the scaled equation of roll motion for a simple harmonic wave is,

$$\ddot{\phi} + D(\dot{\phi}) + R(\phi) = B + \overline{F}\cos(\Omega\tau) \quad (1)$$

with $\Omega = \frac{\omega}{\omega_n}$, $\tau = \omega_n t$ and $\overline{F} = \frac{I}{I+\epsilon I}\frac{Ak\Omega^2}{\phi_v}$

where ϕ represents the scaled roll angle (rad) with the roll rate of $\dot{\phi}$ (rad/s) and the acceleration of $\ddot{\phi}$ (rad/s^2). $D(\dot{\phi})$ is the scaled damping function, $R(\phi)$ is a scaled polynomial that approximates the restoring curve, B is a constant bias moment which might be due to a steady wind or an imbalance in cargo load, $\overline{F}$ is the amplitude of the scaled external periodic force, τ represents the non-dimensional time, ω is the excitation frequency (rad/s), ω_n is the natural angular frequency (rad/s), Ω describes the ratio of excitation to natural frequency, I is the rotational moment of inertia, ϵI is the added moment of inertia due to the surrounding fluid, ϕ_v is the vanishing angle in still water for the initially symmetric GZ (righting arm) and Ak is the wave slope (Bikdash et al., 1994; Spyrou et al., 2000; Spyrou et al., 2002).

For the uncoupled rolling motion under periodic waves, the governing equation (1) is described by the following SDOF (single-degree-of-freedom) model:

$$[I_{44} + A_{44}]\ddot{\phi} + B_{44}\dot{\phi} + \triangle\overline{GZ}(\phi) = F_{sea}(t) \quad (2)$$

where I_{44} is the moment of inertia ($kg.m^2$) of the vessel about the roll axis, A_{44} is the hydrodynamic added mass coefficient ($kg.m^2$), B_{44} is the linear roll hydrodynamic and viscous damping coefficient ($kg.m^2/s$), $\triangle$ is the displacement of the vessel, $\overline{GZ}(\phi)$ is a polynomial approximation to the roll restoring moment curve, F_{sea} denotes the wave exciting moment from beam seas, and the derivatives are denoted with respect to dimensional time t (Jiang et al., 1996).

The mathematical treatment is simplified by approximating the diagram by an odd-order polynomial. The nonlinear restoring arm (moment curve) can be approximated by following the linear and cubic polynomials of ϕ:

$$\overline{GZ}(\phi) = -C_1\phi + C_3\phi^3 \quad (3)$$

where C_1 is the coefficient of linear restoring moment and C_3 is the nonlinear coefficient. This linear-plus-cubic approximation is reliable only for moderate values of the roll angle (< 35°) (Malara et al., 2014). For small angle rolling, the linear restoring term is dominant. On the other hand, the nonlinear term is effective as the roll angle increases (Wu and McCue, 2008). It is clear that at least a fifth-order polynomial is needed to precisely describe the $\overline{GZ}(\phi)$ curve around loll angle and to the angle of vanishing stability (Falzarano, 1990).

The damping moment term is difficult to quantify because these components are coupled with each other (Chai et al., 2016). In fact, the roll damping moment depends on many factors such as the speed, the vessel profile, anti-roll fins and bilge keels (Bikdash et al., 1994). Moreover, a cubic typed viscous damping term may be added to the equation (2) as:

$$[I_{44}+A_{44}]\ddot{\phi}+B_{44}\dot{\phi}+B_{44n}\dot{\phi}^3-C_1\triangle\phi+C_3\triangle\phi^3=F_{sea}(t) \qquad (4)$$

where B_{44_n} is the cubic damping coefficient for nonlinear damper. In addition, A_{44}, B_{44}, B_{44n} and excitation $F_{sea}(t)$ are calculated by the commercial hydrodynamic SHIPMO program (Jiang et al., 1996). This program is based on the strip theory, providing dynamical behaviors of vessels in the frequency domain. The roll excitation in beam seas can be expressed in the following form:

$$F_{sea}(t)=HF_{roll}(\omega)\cos(\omega t) \qquad (5)$$

where F_{roll} is the rolling moment amplitude $(N.m)$ per unit wave amplitude at frequency ω and H is the wave amplitude (Jiang et al., 1996). The excitation harmonic function has the period of $T=2\pi/\omega$ $(s/cycle)$ and the frequency (Hz) of $f=1/T$. From Wang (2010) and Liu et al. (2007), equation (4) can be scaled into a non-dimensional homoclinic equation form using perturbation parameter δ:

$$\frac{\omega_n^2(I_{44}+A_{44})}{C_1\triangle}\ddot{x}+\frac{\omega_n B_{44}}{C_1\triangle}\dot{x}+\frac{\omega_n^3 B_{44n}}{C_1\triangle}\dot{x}^3-x+\frac{C_3}{C_1}x^3 = \frac{HF_{roll}(\omega)}{C_1\triangle}\cos(\Omega\tau) \qquad (6)$$

with $x(\tau)=\phi(t)$, $\tau=\omega_n t$ and $\Omega=\dfrac{\omega}{\omega_n}$. Then, the simplified expression can be obtained from:

$$\ddot{x}+\delta b_{1\delta}\dot{x}+\delta b_{2\delta}\dot{x}^3-x+kx^3=\delta F_\delta\cos(\Omega\tau) \qquad (7)$$

where

$$\delta b_{1\delta}=\frac{B_{44}}{\omega_n(I_{44}+A_{44})}=\frac{\omega_n B_{44}}{C_1\triangle},\qquad \omega_n=\sqrt{\frac{C_1\triangle}{I_{44}+A_{44}}}$$

$$\delta b_{2\delta}=\frac{\omega_n B_{44n}}{I_{44}+A_{44}}=\frac{B_{44n}\sqrt{C_1\triangle}}{(I_{44}+A_{44})^{3/2}},\qquad k=\frac{C_3}{C_1}$$

$$\delta F_\delta=\frac{HF_{roll}}{\omega_n^2(I_{44}+A_{44})}=\frac{HF_{roll}}{C_1\triangle}.$$

By having $\delta b_{1\delta}=b_1$, $\delta b_{2\delta}=b_2$, and $\delta F_\delta=F$, the scaling parameter δ is only used for the theoretical derivation and does not affect dynamical results (Su and Falzarano, 2013). It is a small bookkeeping device artificially introduced to help clarify the order of magnitude of the damping and excitation terms (Bikdash et al., 1994; Roberts and Vasta, 2000). In the above equation, b_1 and b_2 control the amount of damping, k controls the amount of non-linearity in the restoring force, and F is the amplitude of the periodic driving force.

3. Simulation Tests

In this numerical analysis, the nonlinear dynamical characteristics are demonstrated such as equilibrium, stability, periodicity with limit cycle, bifurcations and chaos. The data of the calm dredge, Patti-B (Jiang et al., 1996) is used for our numerical study, as listed in Table 1. Patti-B capsized due to the combined effects of water trapped on its deck. Equation (7) has been numerically integrated with the fourth-order Runge-Kutta method with a time step of $\triangle t=0.005$(s) since the simulation results are comparatively stable over time if the step size is less than this value. An improper selection of time step could eventually lead to numerical instability (Lee and You, 2018). The phase portraits, time history curves and bifurcation diagram of a vessel are extensively described in this section. Numerical integration is the only way to obtain information about the trajectory because most nonlinear differential equations are not soluble analytically. Bifurcation techniques are applied to investigate how the rolling motion changes as the control parameter of frequency ratio Ω is changed. Considering the values of the state variables x and $\dot{x}$, bifurcation diagrams (variable x versus control parameter Ω) of the vessel model are depicted in Fig. 2. In addition to the bifurcation diagram, time history curves and phase portraits are displayed in Fig. 3. The time series shows x as a function of t and the phase portrait depicts the time series plotted in the $x-\dot{x}$ phase plane. The abscissa in Figs 3 (a), (c), (e), (g), (i) and (k) means roll angle (rad) and the ordinate denotes the roll rate of $\dot{\phi}$ (rad/s). The phase portrait provides a lot of information on the behaviors of a dynamical system.

Fig. 2 (a) is the bifurcation diagram obtained by varying Ω from 0.1 to 1.8 for $F=0.5$. In order to show the different periodic motions between chaotic clouds of dots, the magnification zooms of a part of Fig. 2 (a) are depicted in Figs. 2 (b), (c) and (d) in the range of frequency ratio $\Omega=0.32-0.85$. On increasing the value of Ω, one can see chaotic behavior interspersed with intermittent periodic windows. The chaotic region is widely spread at system parameter Ω in the range of about 0.1 to 0.9. When the value of the control parameter is increased beyond the chaotic solution's region, periodic solutions of the model are dominant in the range of $\Omega = 1.01 - 1.6$. It is interesting to note that the different types of sub-harmonic motions (or periodic-orbit families) such as $2T$, $3T$, $4T$, $5T$ exist in the range of frequency ratio $\Omega = 0.34 - 0.83$, illustrating bifurcations eventually leading to chaos.

In order to understand the bifurcation diagram, we illustrate the phase portraits and time series curves in Fig. 3. In the case that $\Omega = 0.34$, one can see a period-4 oscillations with a time period of 19 seconds, as shown in Figs. 3 (a) and (b). Also, Figs. 3 (c) and (d) depict period-3 oscillations and time series for $\Omega = 0.43$. Figs. 3 (e) and (f) illustrate the system responses to be sub-harmonics with a time period of 9.5 seconds for $\Omega = 0.66$. Figs. 3 (g) and (h) depict chaotic behaviors in the case of $\Omega = 0.69$. In general, the chaotic solutions reveal wandering solutions of irregularly oscillating types without a uniform pattern. For the frequency ratio of close to $\Omega = 0.83$, the stable solutions of the period-5 oscillation window appear with a time period of 23 seconds, as shown in Fig. 3 (i) and (j). From the Figs. 3 (k) and (l), it can be seen that the dynamical response is periodic and the phase plane plot is symmetrical with a time period of 6.3 seconds for $\Omega = 1.01$.

Table 1. Numerical data for model parameters (Patti-B)

Parameters	Value
L, vessel length	22.9 m
$\triangle$, vessel displacement	0.237 × 10^7 N
C_1, linear restoring arm	0.214 m
C_3, nonlinear restoring arm	-0.671 m
$I_{44}+A_{44}$, mass moment of inertia	0.147 × 10^7 $kg \cdot m^2$
ω_n, natural angular frequency	0.587 rad/s
B_{44}, linear damping	0.321 × 10^4 $kg \cdot m^2/s$
B_{44n}, nonlinear damping	0.988× 10^5 $kg \cdot m^2/s$
b_1, non-dimensional value	0.0037
b_2, non-dimensional value	0.0672
k, non-dimensional value	3.1355

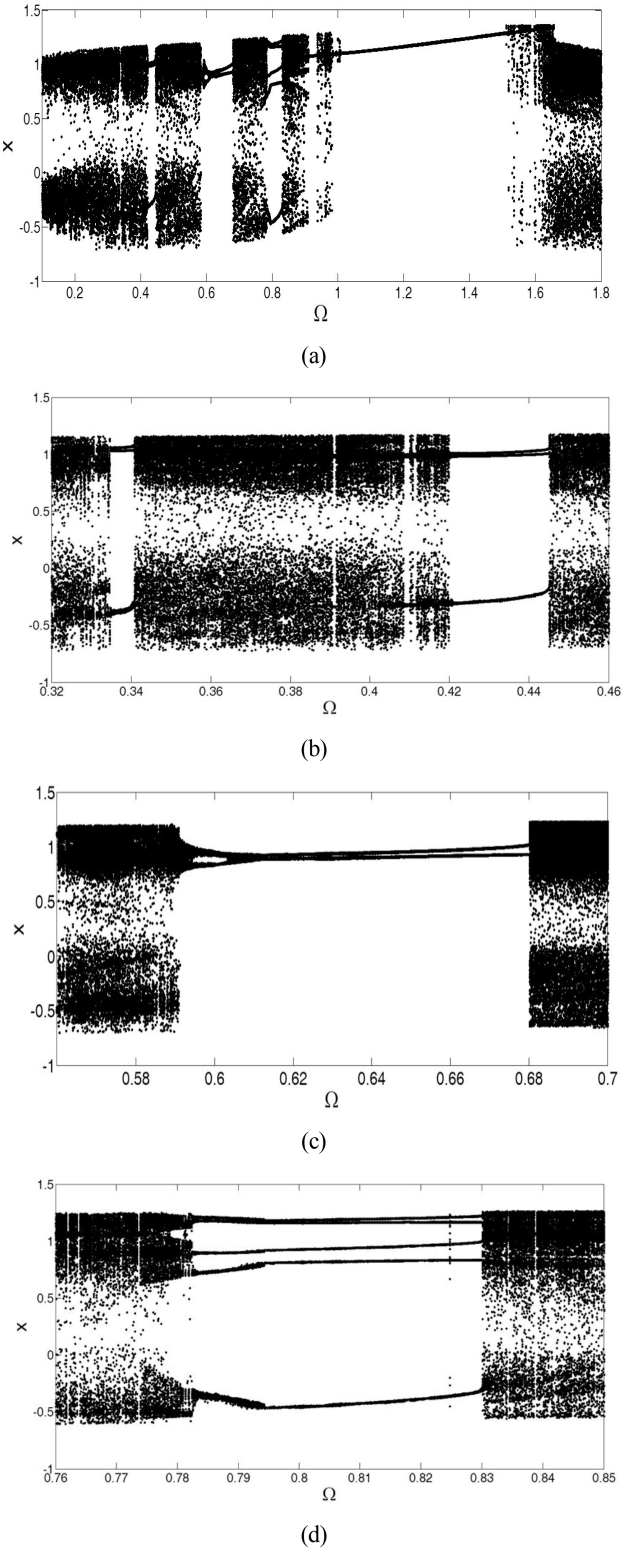

Fig. 2. Bifurcation analysis: (a) bifurcation diagram varying Ω from 0.1 to 1.8 for F=0.5; (b), (c) and (d) magnification of a part of the bifurcation diagram of Fig. 2 (a).

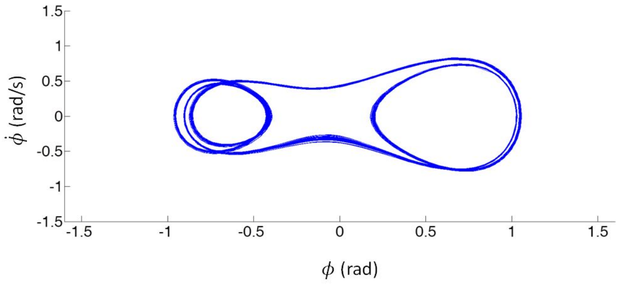

(a) frequency ratio Ω=0.34

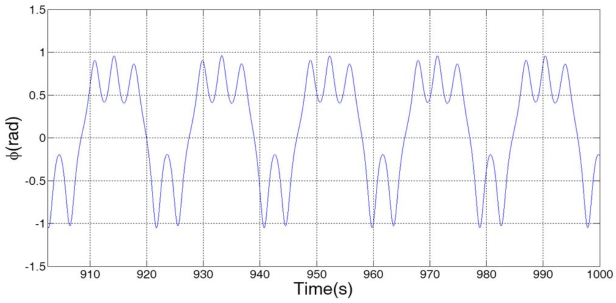

(b) time series for frequency ratio Ω=0.34

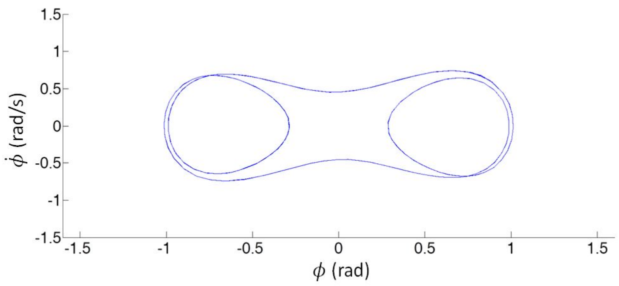

(c) frequency ratio Ω=0.43

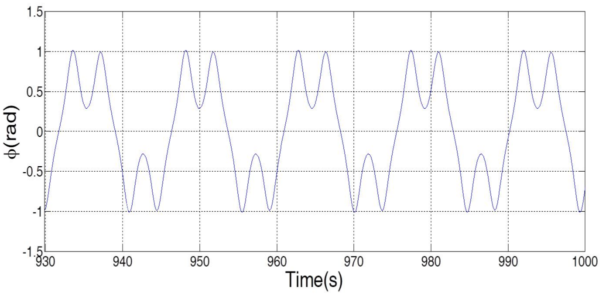

(d) time series for frequency ratio Ω=0.43

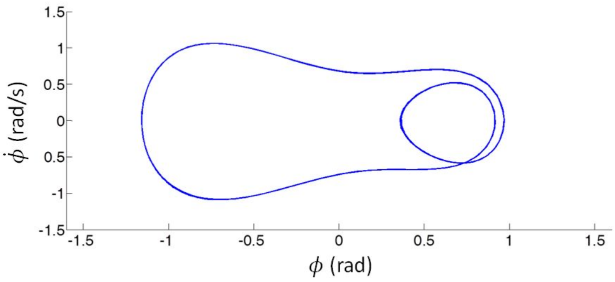

(e) frequency ratio Ω=0.66

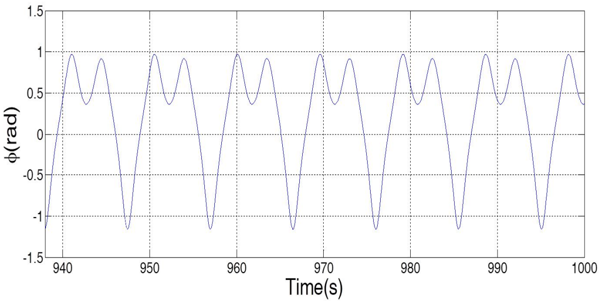

(f) time series for frequency ratio Ω=0.66

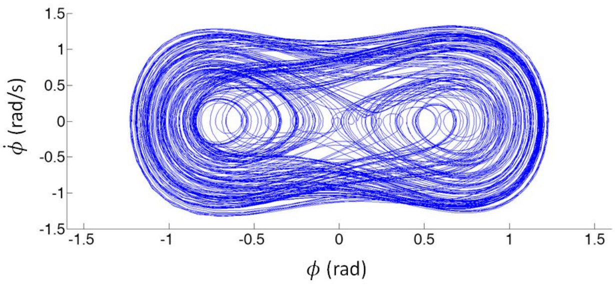

(g) frequency ratio Ω=0.69

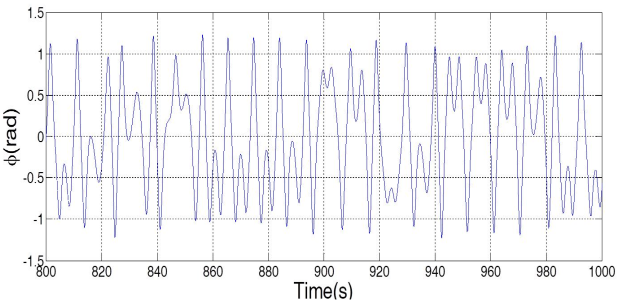

(h) time series for frequency ratio Ω=0.69

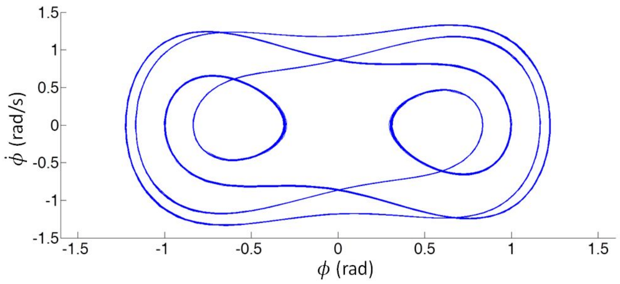

(i) frequency ratio Ω=0.83

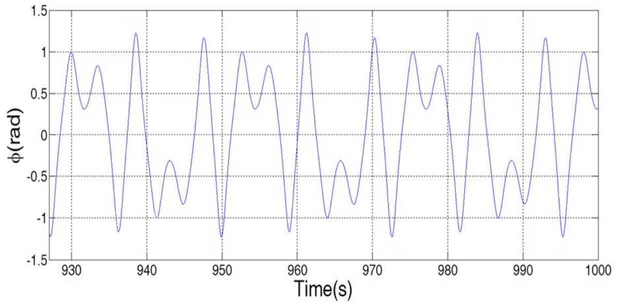

(j) time series for frequency ratio Ω=0.83

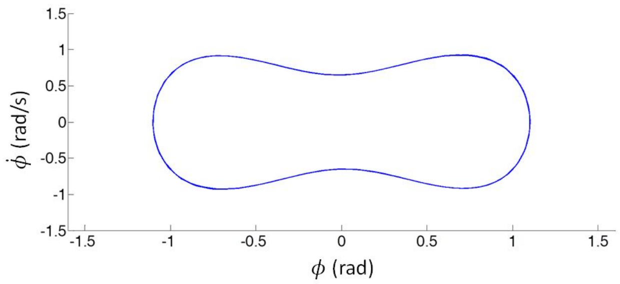

(k) frequency ratio Ω=1.01

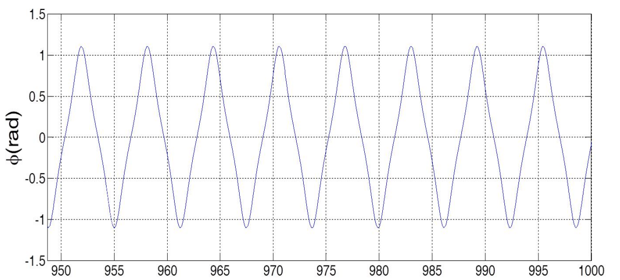

(l) time series for frequency ratio Ω=1.01

Fig. 3. Phase portraits and time history curves varying Ω (0.34, 0.43, 0.66, 0.69, 0.83 and 1.01) for F=0.5.

4. Conclusions

Nonlinear dynamical analysis of a vessel in regular beam waves have been extensively studied in this paper. Periodic, sub-harmonic (periodic-orbit families), limit cycle, and chaotic motion are depicted in the phase plane. Particularly, the bifurcation diagram is used to show the range in detail where nonlinear phenomena are observed under the variations of control parameters.

1) In the range of frequency ratio $\Omega = 0.34 - 0.83$, different types of stable sub-harmonic families exist, such as $2T$, $3T$, $4T$ and $5T$.

2) On increasing frequency Ω, one can see chaotic behaviors interspersed with intermittent periodic windows. The chaotic region is widely spread at system parameter Ω in the range about 0.1 to 0.9. It is found that the rolling motions show complicated dynamical behaviors in regular beam waves.

3) When the value of the control parameter is increased beyond the chaotic region, periodic solutions of the model are dominant in the range of frequency ratio $\Omega = 1.01 - 1.6$.

Finally, this paper presents the qualitative behaviors of the rolling motion in beam waves. It is very important to note that various nonlinear phenomena can be observed according to the slight variations of parameter. More practical systems including coupled roll, pitch, sway and heave will be considered in future studies.

References

[1] Bhattacharyya, R.(1978), Dynamics of Marine Vehicles, John Wiley & Sons Press, pp. 208-219.

[2] Bikdash, M., B. Balachandran and A. Nayfeh(1994), Melnikov Analysis for a Ship with a General Roll-Damping Model, Nonlinear Dynamics, Vol. 6, No. 1, pp. 101-124.

[3] Chai, W., A. Naess and B. J. Leira(2016), Stochastic Nonlinear Ship Rolling in Random Beam Seas by the Path Integration Method, Probabilistic Engineering Mechanics, Vol. 44, pp. 43-52.

[4] Falzarano, J. M.(1990), Predicting Complicated Dynamics Leading to Vessel Capsizing, Doctoral Dissertation, The University of Michigan, pp. 58-181.

[5] Francescutto, A. and G. Contento(1999), Bifurcations in Ship Rolling: Experimental Results and Parameter Identification Technique, Ocean Engineering, Vol. 26, pp. 1095-1123.

[6] Jiang, C., A. W. Troesch and S. W. Shaw(1996), Highly Nonlinear Rolling Motion of Biased Ships in Random Beam Seas, Journal of Ship Research, Vol. 40, No. 2, pp. 125-135.
[7] Jordan, D. W. and P. Smith(2007), Nonlinear Ordinary Differential Equations: An Introduction for Scientists and Engineers, 4th Edition, Oxford University Press, pp. 223-258.
[8] Kamel, M. M.(2007), Bifurcation Analysis of a Nonlinear Coupled Pitch-Roll Ship, Mathematics and Computers in Simulation, Vol. 73, pp. 300-308.
[9] Lee, S. D. and S. S. You(2018), Dynamical Analysis of the Mooring Vessel System Under Surge Excitations, Journal of the Korean Society of Marine Environment & Safety, Vol. 24, No. 2, pp. 140-145.
[10] Lin, H. and S. C. S. Yim(1995), Chaotic Roll Motion and Capsize of Ships under Periodic Excitation with Random Noise, Applied Ocean Research, Vol. 17, pp. 185-204.
[11] Liu, L. Q., Y. G. Tang and H. X. Li(2007), Stochastic Chaotic Motion of Ships in Beam Seas, Journal of Marine Science and Technology, Vol. 15, No. 2, pp. 123-128.
[12] Malara, G., P. D. Spanos and F. Arena(2014), Maximum Roll Angle Estimation of a Ship in Confused Sea Waves via a Quasi-Deterministic Approach, Probabilistic Engineering Mechanics, Vol. 35, pp. 75-81
[13] Neves, M. A. S., N. A. Perez and L. Valerio(1999), Stability of Small Fishing Vessels in Longitudinal Waves, Ocean Engineering, Vol. 26, pp. 1389-1419.
[14] Robets, J. B. and M. Vasta(2000), Markov Modelling and Stochastic Identification for Nonlinear Ship Rolling in Random Waves, Philosophical Transactions of the Royal Society A, Vol. 358, No. 1771, pp. 1917-1941.
[15] Sayed, M. and Y. S. Hamed(2011), Stability and Response of a Nonlinear Coupled Pitch-Roll Ship Model Under Parameter and Harmonic Excitations, Nonlinear Dynamics, Vol. 64. pp. 207-220.
[16] Spyrou, K. J., B. Cotton and J. M. T. Thompson(2000), Nonlinear Dynamics of Ship Rolling in Beam Seas and Ship Design, Contemporary Ideas on Ship Stability, Elsevier Science, pp. 499-510.
[17] Spyrou, K. J., B. Cotton and B. Gurd(2002), Analytical Expressions of Capsize Boundary for a Ship with Roll Bias in Beam Waves, Journal of Ship Research, Vol. 46, No. 3, pp. 167-174.
[18] Strogatz, S. H.(1994), Nonlinear Dynamics and Chaos, 1st Edition, Perseus Books Publishing, pp. 44-45.
[19] Su, Z. and J. M. Falzarano(2013), Markov and Melnikov Based Method for Vessel Capsizing Criteria, Ocean Engineering, Vol. 64, No. 15, pp. 146-152.
[20] Wang, Y. G.(2010), Melnikov Analysis of a Ship's Stability with Water-on-Deck, Journal of Marine Science and Technology, Vol. 18, No. 1, pp. 106-111.
[21] Wu, W. and L. MeCue(2008), Application of the Extended Melnikov's Method for Single-Degree-of-Freedom Vessel Roll Motion, Ocean Engineering, Vol. 35, No. 17-18, pp. 1739-1746.
[22] Zhou, L. and F. Chen(2008), Stability and Bifurcation Analysis for a Model of a Nonlinear Coupled Pitch-Roll Ship, Mathematics and Computers in Simulation, Vol. 79, pp. 149-166.

Received : 2018. 04. 30.
Revised : 2018. 05. 27.
Accepted : 2018. 05. 29.